



Research paper

Electrical, dielectric and electrochemical characterization of novel poly(acrylic acid)-based polymer electrolytes complexed with lithium tetrafluoroborate

Koh Sing Ngai^a, S. Ramesh^{a,*}, K. Ramesh^a, Joon Ching Juan^b

^a Centre for Ionics University of Malaya, Department of Physics, Faculty of Science, University of Malaya, 50603 Kuala Lumpur, Malaysia

^b Nanotechnology & Catalysis Research Centre (NANOCAT), Institute of Postgraduate Studies (IPS), University of Malaya, 50603 Kuala Lumpur, Malaysia

ARTICLE INFO

Article history:

Received 22 September 2017

In final form 20 November 2017

Available online 29 November 2017

Keywords:

Poly(acrylic acid)

Lithium tetrafluoroborate

Polymer electrolyte

Ionic conductivity

Dielectric permittivity

ABSTRACT

A series of novel poly(acrylic acid)-based polymer electrolytes with high conductivities at room temperature has been prepared and studied. Polymer electrolytes composed of poly(acrylic acid) (PAA) and lithium tetrafluoroborate (LiBF_4) were prepared by means of solution casting. The effect of the addition of LiBF_4 on the properties of the PAA-based electrolyte matrices was analysed and investigated using impedance spectroscopy. The optimized PAA-based solid electrolyte showed an electrochemical stability window of 3.2 V. Thermogravimetric analysis indicated that the incorporation of LiBF_4 into PAA matrix enhances the thermal stability. The structural properties of polymer electrolytes were studied by using X-ray diffraction analysis.

© 2017 Elsevier B.V. All rights reserved.

1. Introduction

Liquid electrolytes are used in the production of batteries and other electrical devices for the past few decades. There are shortcomings of conventional liquid electrolytes such as internal shorting, and potential leaking of corrosive solvent and harmful liquid or gas [1,2]. In 1973, polymer electrolyte was introduced by Fenton et al. [3]. Solid polymer electrolytes have several inherent advantages over the conventional liquid electrolytes. Polymer electrolytes have drawn a great deal of attention due to their technological applications in advanced electrochemical devices such as capacitors, batteries, electronics and electrochromic devices [1,2,4]. These polymer electrolytes possess interesting properties over their liquid counterparts such as flexibility for various shape configuration and thin-film forming ability [5,6]. At the same time, polymer electrolytes are used as separators in lithium-ion and lithium-polymer batteries due to their chemical and thermal properties. Other inherent advantages and promising features of the polymer electrolytes make them widely used in the battery application [7].

The development of new polymer electrolytes with enhanced features and characteristics has become an important research area in the recent years. A polymer electrolyte is composed of at least one inorganic salt embedded in a host polymer matrix [8,9].

Examples of host polymers that are widely used in the preparation of polymer electrolytes in previous literatures such are poly(ethylene oxide) (PEO) [10,11], poly(vinyl chloride) (PVC) [12,13], poly(vinylidene fluoride) (PVdF) [14,15], polymethyl methacrylate (PMMA) [16,17], and poly(acrylic acid) (PAA) [18,19]. Many polymers are non-ionic or electronic conductors in nature. The dissociation of salt trapped in the polymer system allows conductivity through the mobile ions. It will be interesting to study and characterize the effects of various temperatures and concentrations of inorganic salts on the conductivity of the polymer electrolytes. Dielectric study is a versatile study to characterize the electrical properties of dielectric materials such as polymer electrolytes. It investigates the dielectric relaxation behaviour of dipoles in polymer electrolytes. Dielectric permittivity in a polymer electrolyte is measured to demonstrate the complex dielectric behaviour. A measurement of dielectric permittivity refers to the relaxation response of a dielectric material to an external electrical field as a function of frequency. It also represents the stored and lost charges in a material. The charge carriers in solid polymer electrolytes are mainly ions. Like ionic conductivity, dielectric study of polymer electrolytes can be determined by AC-impedance spectroscopy over a wide range of frequency.

In this study, we have studied the electrical and dielectric properties of novel PAA-based solid electrolyte systems with different weight percentage of lithium salt. PAA was reported to be biodegradable, with a good processability and mechanical strength [18,20]. The promising features of PAA make it a vital

* Corresponding author.

E-mail address: ramesh@um.edu.my (S. Ramesh).

material to be used as a host polymer in a new polymer electrolyte system. The polymer film with lithium tetrafluoroborate (LiBF_4) as dopant demonstrated a high ionic conductivity in previous literatures [21,22]. Moreover, a polymer electrolyte prepared of PAA and LiBF_4 has not been reported in any literatures, so far. The ionic conductivity of PAA electrolyte films with different lithium salt composition was investigated by AC-impedance spectroscopy. Three polymer electrolyte systems with the highest ionic conductivity were subjected to the temperature-dependent study. Dielectric studies were also performed for polymer electrolyte systems in low, intermediate and high lithium salt content. The electrochemical stability window for the polymer electrolyte with the highest ionic conductivity was also examined.

2. Experimental

2.1. Chemicals and reagents

Poly(acrylic acid), PAA with an average molecular weight of 450,000 was obtained from Sigma-Aldrich Co., St. Louis, MO, USA and used as a host polymer. Lithium tetrafluoroborate, LiBF_4 (98% in purity) was purchased from Sigma-Aldrich and employed as an inorganic dopant salt. Deionised water was used as the solvent to dissolve all starting materials. All the materials were used as received without further treatment and kept dry in desiccator before use.

2.2. Instrument

The ionic conductivity of the samples with respect to chemical composition and temperature was studied using AC-electrochemical impedance spectroscopy (EIS). The measurement was carried out using HIOKI 3532–50 LCR HiTESTER interfaced to a computer for data acquisition over a frequency range of 50 Hz to 5 MHz. The data were obtained and processed using an appropriate fitting program. The electrochemical stability window of the polymer electrolyte film with the highest ionic conductivity was evaluated using linear sweep voltammetry (LSV) via GAMRY INSTRUMENTS Interface 1000 Potentiostat/ Galvanostat/ZRA at ambient temperature. Thermal stability of polymer electrolyte films was determined by thermogravimetric analysis (TGA) via Simultaneous Thermal Analyzer (STA) 6000. The structural studies of the polymer electrolyte films were examined by X-ray diffraction (XRD) using EMPYREAN X-ray Diffractometer.

2.3. Preparation of polymer electrolytes

All thin films of polymer electrolytes were prepared using solvent casting technique. Prior to the preparation of the polymer electrolytes, LiBF_4 was dried at 100 °C for 1 h to eliminate any trace amounts of water in the material. Several polymer electrolyte complexes were prepared according to the ratio of polymer to lithium salt, ranging from 95/5 to 60/40. Appropriate amounts of PAA and LiBF_4 were dissolved in deionized water. The mixtures were continuously magnetically stirred for 12 h to obtain homogeneous mixtures at 100 °C. The mixtures were then cast on a flat glass and dried in an oven at a proper temperature for at least 12 h to remove the solvent. This procedure yields mechanically stable and free standing films. The dried samples were placed inside plastic bags and stored in a desiccator to avoid moisture contamination. Conductivity measurements indicated that a weight percent ratio of 70/30 for PAA: LiBF_4 yielded the highest conductivity. This composition was therefore used for the electrochemical study.

2.4. Characterization

2.4.1. Ambient temperature-ionic conductivity studies

The ambient temperature-ionic conductivity studies of the polymer electrolyte films were determined by AC-impedance spectroscopy. The samples were removed from the plastic bags and cut into the shape of the stainless steel blocking electrodes used in this study. The samples were then mounted between two parallel stainless steel blocking electrodes and held under the pressure of springs.

The bulk ionic conductivity of the polymer electrolytes was determined by using the following equation:

$$\sigma = \frac{L}{R_b \times A} \quad (1)$$

where σ represents the ionic conductivity (S cm^{-1}), L is the thickness of the polymer film sample (cm), R_b is the bulk resistance obtained from the Cole–Cole impedance plot (Ω), and A is the surface area of the stainless steel blocking electrodes (cm^2). The disk electrode with a diameter of 1.9 cm having a surface area of 2.836 cm^2 . The thickness of the thin films was measured by using a digital micrometer screw gauge.

2.4.2. Chemical composition studies

Ionic conductivity measurement at ambient temperature was carried out on the PAA-based solid electrolyte films composed of different lithium salt percentages, in the range of 5–40 wt%. Table 1 lists the chemical composition analysis for the PAA-hosted electrolyte systems with various LiBF_4 content.

2.4.3. Temperature dependent-ionic conductivity studies

For temperature-dependence ionic conductivity study, the ionic conductivity measurements were taken from ambient temperature to 120 °C at an interval of 10 °C. Samples were kept for 30 min to attain the thermal equilibrium for each temperature tested. All the experimental temperatures were attained by means of a convection oven.

2.4.4. Dielectric studies

Dielectric properties of a polymer electrolyte can be studied via dielectric study. In dielectric study, measurements pertaining to the storage or dissipation of electrical energy in a polymer electrolyte are determined and described in various parameters: dielectric permittivity, dielectric loss, loss tangent, relative permittivity, dielectric constant, dielectric relaxation, and dielectric modulus.

Permittivity of a dielectric material is composed by two components, the real and imaginary parts of a dielectric constant, which is described as:

$$\varepsilon^* = \varepsilon' - i\varepsilon'' \quad (2)$$

Table 1

Chemical composition of PAA-based electrolyte systems with different weight percentage of LiBF_4 at ambient temperature.

Sample	Sample weight (g)	PAA (g)	LiBF_4 (g)	Composition ^a (wt%)
P95-L5	1.0	0.95	0.05	(95:5)
P90-L10	1.0	0.90	0.10	(90:10)
P85-L15	1.0	0.85	0.15	(85:15)
P80-L20	1.0	0.80	0.20	(80:20)
P75-L25	1.0	0.75	0.25	(75:25)
P70-L30	1.0	0.70	0.30	(70:30)
P65-L35	1.0	0.65	0.35	(65:35)
P60-L40	1.0	0.60	0.40	(60:40)

^a PAA: LiBF_4 .

The real component, or dielectric permittivity is expressed by:

$$\epsilon' = \frac{Z_i}{\omega C_0(Z_y^2 + Z_i^2)} \quad (3)$$

and the imaginary component, or dielectric loss is expressed by:

$$\epsilon'' = \frac{Z_y}{\omega C_0(Z_y^2 + Z_i^2)} \quad (4)$$

where Z_y and Z_i are the real and imaginary parts of impedance, respectively. ω is angular frequency in Hertz (Hz), where $\omega = 2\pi f$. C_0 is obtained by the following formula:

$$C_0 = \frac{\epsilon_0 A}{l} \quad (5)$$

where ϵ_0 is the vacuum permittivity (also known as the permittivity of free space, which is equal to $8.854 \times 10^{-12} \text{ F m}^{-1}$), A is the contact area of the electrolyte–electrode interface, l is the thickness of the dielectric sample.

The relative permittivity, ϵ_r (also known as dielectric constant, K) is defined as:

$$\epsilon_r = \frac{\epsilon}{\epsilon_0} \quad (6)$$

Dielectric loss can also be parameterized in terms of long tangent, which is defined as:

$$\tan \delta = \epsilon'' / \epsilon' \quad (7)$$

The real part of modulus, M' and the imaginary part of modulus, M'' are expressed as below:

$$M' = \frac{\epsilon'}{[(\epsilon')^2 + (\epsilon'')^2]} \quad (8)$$

$$M'' = \frac{\epsilon''}{[(\epsilon')^2 + (\epsilon'')^2]} \quad (9)$$

The analyses were performed over the frequency range of 50 Hz to 5 MHz.

2.4.5. Electrochemical stability window

The electrochemical stability window of the polymer electrolyte film was evaluated using linear sweep voltammetry (LSV) at room temperature. A GAMRY electrochemical interface was used for the measurement with the configuration of stainless steel (SS)/polymer electrolyte film/SS. The analysis was performed between -2.5 and $+2.5$ V at a scan rate of 5 mV s^{-1} . The sample interval was 0.001 V with 2 s as the rest time prior to the measurement.

2.4.6. Thermogravimetric analysis

The thermal stability of PAA-LiBF₄ electrolyte systems was investigated using a thermogravimetry analyzer consisting of STA 6000 main unit and Pyris software, version 11. Thin film samples were heated from 30°C to 600°C with a heating rate of $10^\circ\text{C min}^{-1}$ under an inert nitrogen flow rate of 20 ml min^{-1} .

2.4.7. X-ray diffraction studies

The amorphosity of polymer electrolytes was investigated using XRD study with Cu K α radiation of wavelength 1.5406 \AA , scattering over the range of 2θ between 5° and 90° .

3. Results and discussion

3.1. Ambient temperature-ionic conductivity studies

The AC-impedance spectroscopy analysis is a typical method used to measure the ionic conductivity of the polymer electrolyte films. The Cole-Cole plot of PAA-LiBF₄ solid electrolytes is presented in Fig. 1. The bulk resistance (R_b) was determined from the intercept on the real axis at high frequency of the Cole-Cole plot. R_b of 5Ω was obtained from the plot. The thickness of the polymer electrolyte films was measured using Mitutoyo digital gauge. The average thickness obtained was about 0.095 mm . The ionic conductivity of $6.6 \times 10^{-4} \text{ S cm}^{-1}$ was calculated for the polymer electrolytes using the equation described in the Experimental section.

3.2. Chemical composition studies

The optimum composition of PAA-based solid electrolyte is significant for the technological applicability of the polymer system in various electrical/electrochemical devices. In this work, dependence of ionic conductivity on LiBF₄ concentration reveals the effect on the ionic conductivity when lithium salts interact with PAA. The variation of ionic conductivity with polymer electrolytes of different lithium salt content is illustrated in Fig. 2.

The ionic conductivity of the polymer electrolytes increases with lithium salt content. As shown in Fig. 2, P95-L5, the PAA-hosted sample with 5 wt% of LiBF₄, showed the lowest ionic conductivity among all the experimental samples, which was about $2.32 \times 10^{-7} \text{ S cm}^{-1}$ at ambient temperature. On the other hand, P70-L30 achieved the highest conductivity of $6.61 \times 10^{-4} \text{ S cm}^{-1}$ upon the incorporation of 30 wt% of lithium salt. Above 35 wt% of LiBF₄, the casting films were difficult to handle and therefore not appropriate for the experiment. Fig. 2 shows conductivity increases with the loading of LiBF₄ salt. As expected, ionic conductivity is enhanced instantaneously with the incorporation of lithium salt.

At low content of lithium salt, two regions are observed in the spectrum of Cole-Cole plot, namely a linear region in the low frequency range and a semi-circle in the high frequency range. This indicates a considerable high bulk resistance of the systems was achieved. Upon the increase of the lithium salt concentration, the semi-circle becomes obscure and diminishes completely after the addition of 10 wt% of LiBF₄. The polymer electrolyte with 30 wt% of lithium salt shows the typical shape of a very ionic conductive thin film sample, where an electrode spike is clearly seen in the higher frequency region.

Lithium ions in LiBF₄ act as charge carriers. The increase of lithium salt concentration leads to the increase in the number of mobile lithium ions. The increase of ionic conductivity in the initial stage was due to the increased availability of lithium ions in the polymer matrix. At higher concentrations of lithium salt, the presence of excessive lithium salt starts to disrupt the crystalline morphology of PAA matrix, and converts it into amorphous phase. The amorphous nature of the polymer matrices often correlates with high ionic conductivity. However, from 35 wt% onwards, ionic conductivity decreases as indicated in Fig. 2. This could be attributed to the re-association of lithium salt, which consequently reduces the availability of freely mobile ions. The tendency of the formation of neutral ion pairs also contributes to the decreasing of ionic conductivity even with the addition of extra lithium salt.

3.3. Temperature dependent-ionic conductivity studies

Ionic conductivity is one of the most important aspect of the polymer electrolytes for determining the ability of the electrolyte

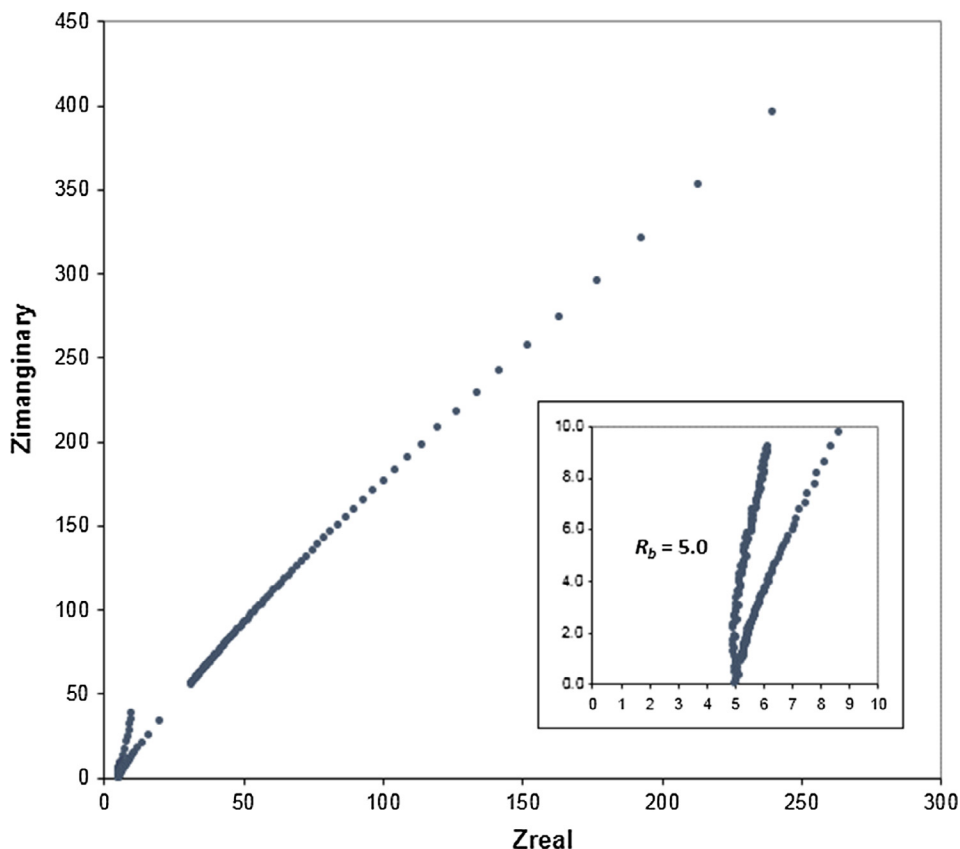


Fig. 1. Cole-Cole plot of PAA-LiBF₄ solid electrolyte films at room temperature. The inset shows the magnified axis of 30 wt% LiBF₄ in a higher frequency region of the real part of complex impedance (x-axis). The imaginary part of complex impedance is the y-axis.

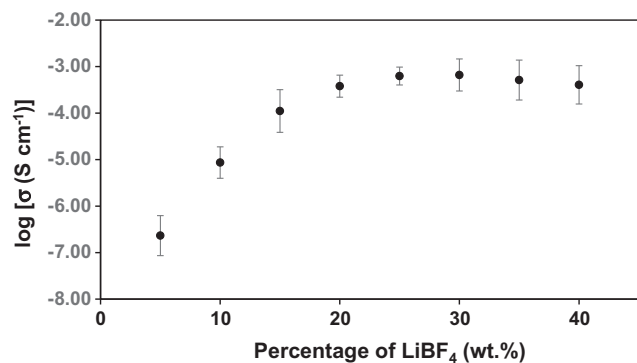


Fig. 2. The variation of ionic conductivity with different lithium salt content in PAA-based electrolyte systems.

systems to generate current. In order to be used as a separator in an electrochemical device, a polymer electrolyte must possess high ionic conductivity associated with other desirable features like wide electrochemical window, good thermal stability, and good mechanical property. Electrochemical impedance spectroscopy is commonly used to compute ionic conductivity. Ionic conductivity varies with several factors, for instance, temperature, types of anions and cations, concentration of salt, types of additives, etc. In this study, the temperature-dependent conductivity measurement was carried out in the temperature ranging of 303–393 K in order to analyze the ionic conduction mechanism in the polymer electrolyte systems.

When 30 wt% of lithium salt was incorporated into the polymer electrolyte, the highest ionic conductivity of $6.6 \times 10^{-4} \text{ S cm}^{-1}$ was

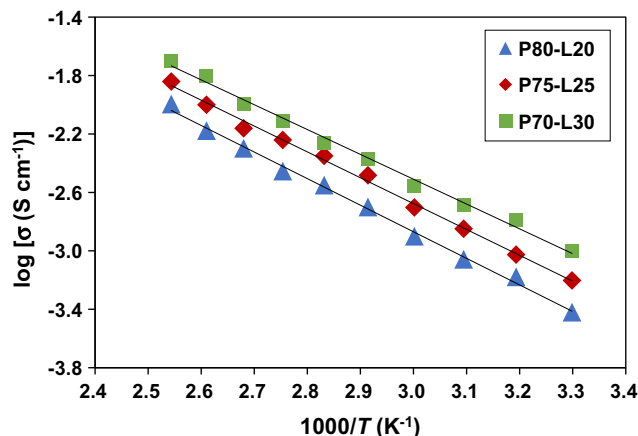


Fig. 3. The variation of logarithm ionic conductivity as a function of inverse absolute temperature from 303 K to 393 K.

achieved at ambient temperature, as illustrated in Fig. 3. Results confirm the increase of ionic conductivity with the increase in temperature. This is due to the increase in temperature which can be demonstrated using Arrhenius plot. It was observed that all the tested polymer electrolyte films obey the Arrhenius theory which reveal that ion conduction mechanism is thermally assisted. When the temperature of the polymer matrices is increased, the mobile ions acquire more energy which allows faster motion. The mobile ions jump into neighbouring vacant sites. This is attributed to the decrease in the crystallinity in the PAA-LiBF₄ electrolyte matrix that facilitates fast motion of lithium ions in the polymer network. It was suggested that the lower activation energy of a polymer

electrolyte is coupled with higher ionic conductivity. The activation energy (E_a) for the polymer electrolyte system with 30 wt% of LiBF_4 is 3.4×10^{-4} eV. The decrease in activation energy shows that the amorphocity of the PAA- LiBF_4 electrolyte systems enables the lithium ions to move faster inside the polymer matrix. The activation energy of P70-L30 was lower than P80-L20 which needed less energy for the mobility of charge carriers and thus led to higher ionic conductivity.

3.4. Dielectric permittivity study

Fig. 4(a) and (b) illustrate the frequency dependence variation of dielectric permittivity and dielectric loss, respectively, for P90-L10, P80-L20, and P70-L30. As can be seen from the figures, all three polymer electrolyte systems exhibit similar observations. There is a rapid fall in the lower frequency range for all three systems. This is due to the electrode polarization when electrical field was applied across the samples [23]. The mobile charge carriers were attached at the electrode-electrolyte interface. In the higher frequency range, the readings decreased and saturated, whereby there were no significant changes. This feature is commonly observed in the permittivity plots for polymer electrolyte systems. As explained by Awadhia et al., the decrease in dielectric permittiv-

ity with higher frequency could be attributed to the inability of dipoles to rotate rapidly which lead to the lag between frequency of oscillating dipole and the applied field [24].

Fig. 4(a) and (b) also show that dielectric permittivity increases with the increase of the amount of inorganic salts in the polymer electrolyte matrices. P70-L30 showed the highest dielectric permittivity and P90-L10 showed the lowest dielectric permittivity at a particular frequency. However, polymer electrolytes are also associated with the comparatively higher dielectric loss than others. The higher dielectric permittivity in polymer electrolytes with higher inorganic salt content is associated to the number of charge carriers. As the inorganic salt content increases, the density of the charge carriers (mobile ions) is also increased. This can lead to the increase in charges stored in the sample [25].

3.5. Loss tangent

The enhancement of ionic conductivity in polymer electrolytes is always coupled with two main factors: the mobility of charge carriers (cations), and the concentration of conducting cations. Both information can be established by the plots of frequency dependence of loss tangent study. The plot of loss tangent against angular frequency reveals the insight on the extent of mobile ions transportation in polymer electrolyte matrices in different inorganic salt content. The area under the peak of the plot correlates to the number of ions involved in the relaxation process.

Fig. 5 demonstrates the displacement of peaks of tangent loss when inorganic salt content increases from 10 to 30 wt%. Based on Fig. 5, the tangent loss peak for P90-L10 is slightly shifted to a lower frequency compared to P70-L30. The relaxation frequencies for polymer electrolyte samples with different inorganic salt content are summarized in Table 2. The peak of polymer electrolytes with lower inorganic salt content at a relatively lower frequency side compared to others is correlated to its slightly slow cations mobility. On addition of inorganic salt, the peak shifts toward a higher frequency. This behaviour suggests the speed up of relaxation time. The increase of inorganic salt content correlates to the enhancement in the amorphocity of the matrix, which endorsing more sites for cations mobility. This reduces the relaxation time which leads to the displacement of peaks to a higher frequency. The results clearly illustrate that ionic conductivity is

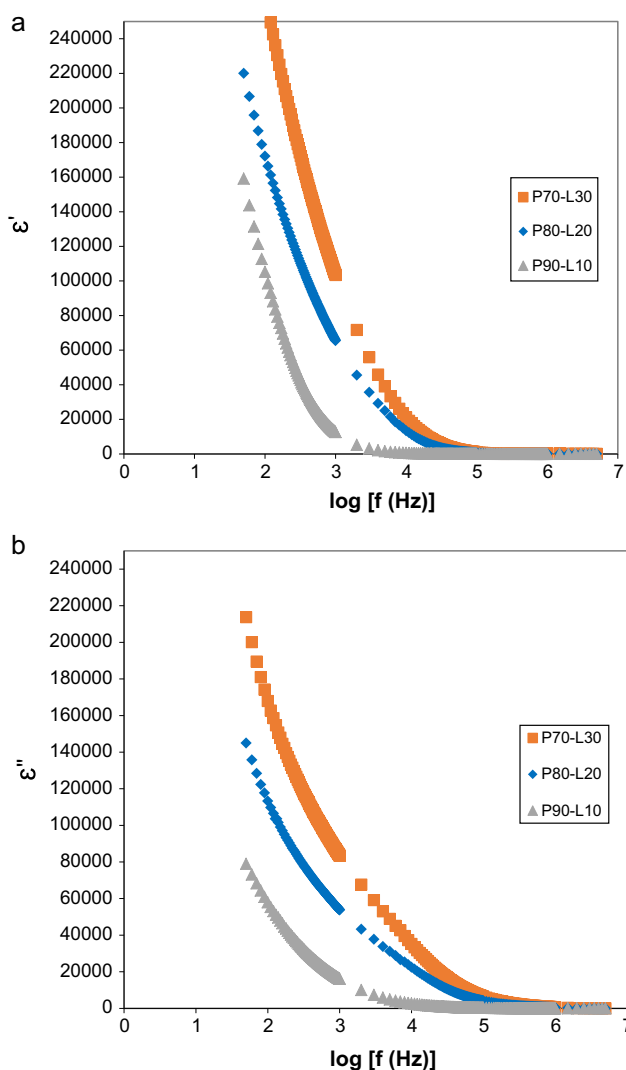


Fig. 4. Variation of (a) dielectric permittivity and (b) dielectric loss for P90-L10, P80-L20, and P70-L30 as a function of frequency at ambient temperature.

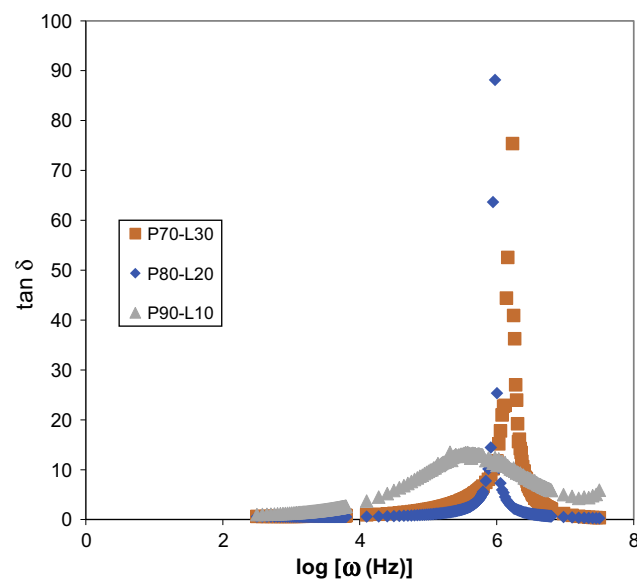


Fig. 5. The frequency dependence variation of loss tangent for P90-L10, P80-L20, and P70-L30.

Table 2

Relaxation frequencies for different polymer electrolyte samples with various inorganic salt contents.

PE sample	Relaxation frequency, $\log \omega_m$ (Hz)
P70-L30	6.2
P80-L20	6.0
P90-L10	5.6

dependent on the mobility of charge carriers, as well as the concentration of conducting cations.

3.6. Modulus studies

Dielectric modulus study is another approach to study the dielectric relaxation behaviour by suppressing electrodes' polarization effect. The real part of dielectric modulus (M') and the imaginary part of dielectric modulus (M'') of different polymer electrolytes are shown in Fig. 6(a) and (b), respectively. In these figures, the relaxation peaks are absent. As can be seen from the figures, abrupt increments are observed in the higher frequency range. At a lower frequency regime, both P80-L20 and P70-L30 indicate long tail prior leading to the zero end. The long tail reveals the suppression of the electrical double layer effect at the contact of electrode-electrolyte area [26]. As described in the literatures, the suppression of electrical double layer is associated with a high capacitance value with the electrode in the polymer electrolyte systems [27].

3.7. Electrochemical stability window

The electrochemical stability window of the polymer electrolytes was determined with linear sweep voltammetry (LSV) in the potential range of -2.5 to $+2.5$ V at a scan rate of 5 mV s^{-1} . LSV responses of the stainless steel electrode/polymer electrolyte cell assembly are shown in Fig. 7. It was found that PAA-based electrolyte systems exhibited an anodic stability up to 3.2 V, in the potential range from -1.5 to $+1.7$ V. Beyond the potential range, the polymer electrolytes start to be degraded. As stated by Kotz & Carlen, the electrochemical stability window above 3 V is suitable for the application in electrochemical devices [28]. The oxidation occurring at potentials higher than 3.2 V for PAA-LiBF₄ electrolyte systems makes it suitable for the applications in electrochemical devices. The wider electrochemical stability range of PAA-LiBF₄ systems could be attributed by the electron delocalization of tetrafluoroborate anions, which is induced by the strong electron withdrawing group [29]. The tetrafluoroborate anions undergo electron delocalization processes to form resonance structures. Since the tetrafluoroborate anions achieve a more stable state, it is expected that the electrochemical stability would be improved.

3.8. Thermogravimetric analysis

TGA is a thermal technique to examine the thermal stability of polymer electrolytes under inert condition. The overall thermal properties of the polymer electrolyte systems can be investigated by determining the weight loss of the samples over a selective temperature range at a controlled uniform heating rate. Fig. 8 shows the overlay of four thermograms of pure PAA, P80-L20, P75-L25, and P70-L30 in the temperature range of 30–600 °C. Four stages of significant weight losses were observed upon heating pure PAA. The initial weight loss of 0.5% in the region of 30–144 °C was due to the evaporation of water molecules trapped in PAA film. Decarboxylation that occurs in PAA after prolonged

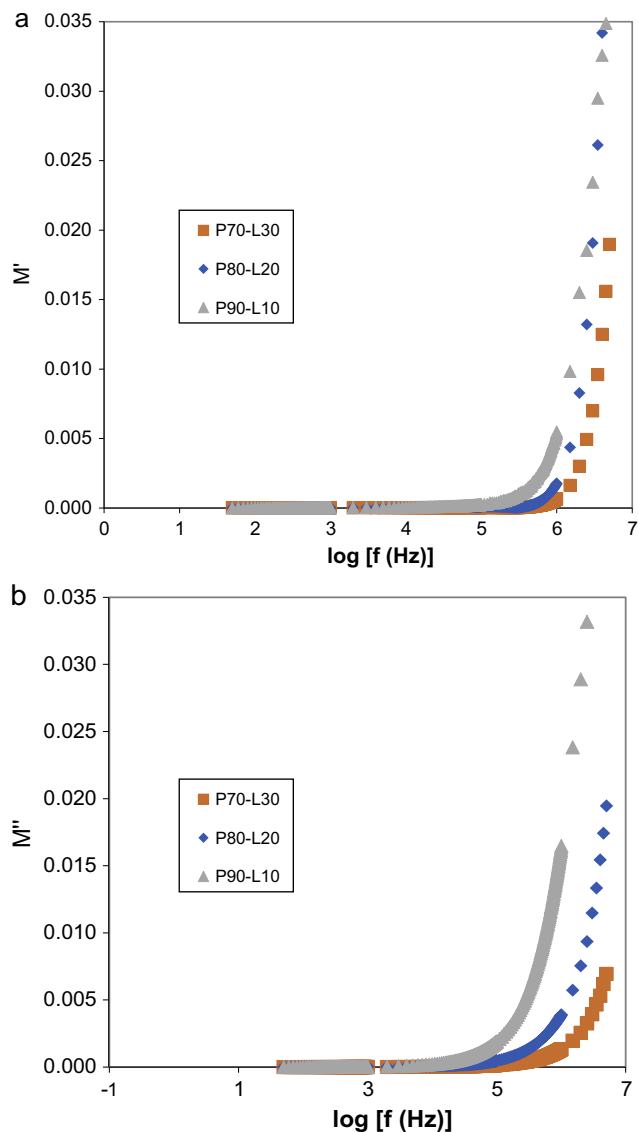


Fig. 6. The (a) real part and (b) imaginary part of dielectric moduli as a function of frequency for P90-L10, P80-L20, and P70-L30.

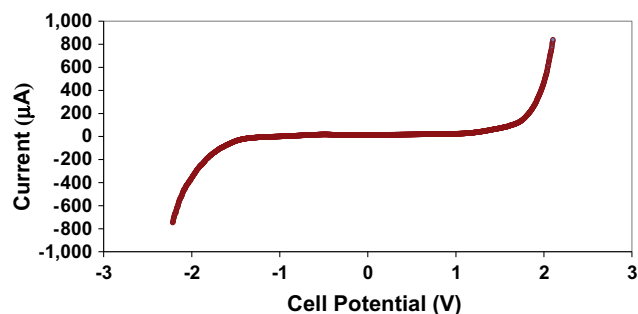


Fig. 7. LSV curve of PAA system with 30 wt% LiBF₄ at ambient temperature. (Scan rate: 5 mV s^{-1}).

heating also leads to weight loss [18]. Below 150 °C, the major reaction which takes place is the formation of intramolecular anhydride [30]. About 11.4% of weight loss was measured in the region of 150–275 °C. In this region, the anhydride concentration

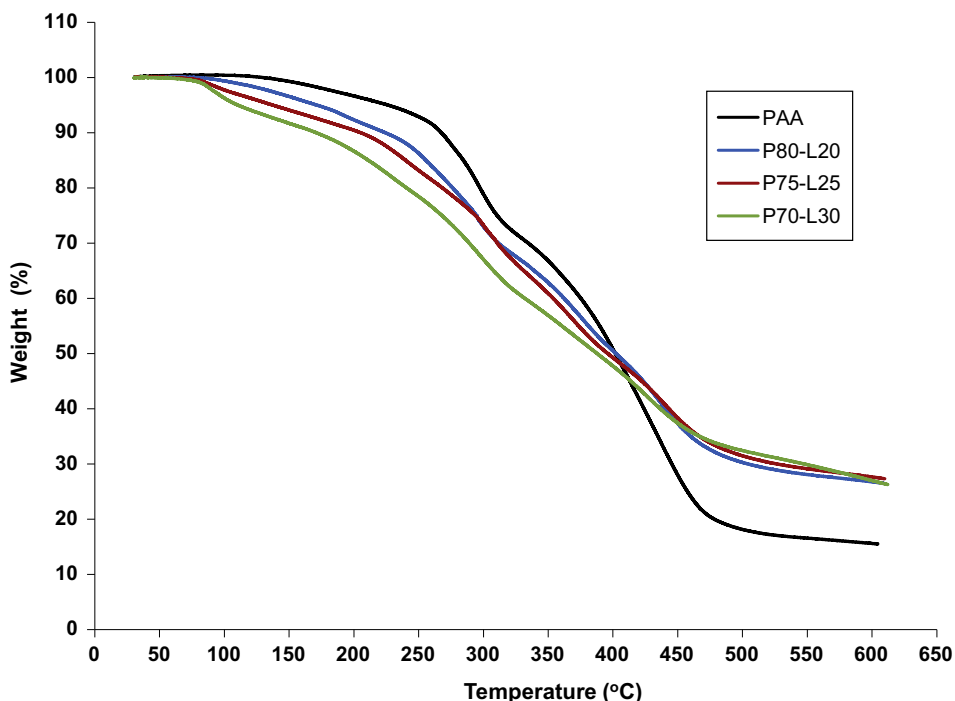


Fig. 8. TGA curves of pure PAA, P70-L30, P75-L25, and P80-L20.

decreased with an overall reduction in acrylic acid content [30]. In the region of 275–350 °C, another drastic reduction in weight was detected. This is due to the formation of cyclic ketone in the decarboxylated PAA chain at higher temperatures [31]. The rapid loss of PAA weight at above 300 °C ascribed to the occurrence of decomposition until a residual mass of 15.5% was achieved.

The initial weight loss of 5% for P70-L30 up to 110 °C is attributed to the loss of water molecules. Water was used as the solvent in the polymer electrolytes systems. Some of the water molecules may have been trapped in small cavities formed in the polymer matrices upon solidification. Under ambient temperature, it is hard to diffuse them out of the polymer matrices. The gradual removal of water molecules from the samples led to the prolonged weight loss between 110 and 200 °C, as indicated in Fig. 8. The addition of hydrophilic LiBF_4 into the polymer electrolyte systems increased the moisture absorption. As shown in Fig. 8, P70-L30 has the higher initial weight loss and P80-L20 has the relatively lower initial weight loss. P70-L30 with 13% weight loss at 200 °C could be attributed to the hydrophilicity of LiBF_4 . P80-L20 has a weight loss of 8% at 200 °C, which indicates P80-L20 has a better thermal stability than P70-L30. The second weight loss between 100 and 150 °C reflects the decarboxylation process. P70-L30, P75-L25 and P80-L20 portray a small weight loss between 2% and 5% in this region. The samples lost weight when subjected to continuous heat between 150 and 300 °C. The third weight loss was a maximum weight loss with a sharp decrease in weight percentage at 244 °C. This ascribes the elimination of ketone compound [18]. Above 300 °C, the degradation of LiBF_4 to form boron trifluoride occurs. The last stage of weight loss between 300 and 450 °C was the decomposition of main polymer chain. The weight loss of polymer electrolytes was improved upon incorporation of LiBF_4 where the total mass loss of pure PAA and P70-L30 are 84.5% and 73.7%, respectively, within the temperature range of 30–600 °C. The higher residual mass of polymer electrolytes at 600 °C could be attributed to the improved thermal stability of polymer electrolyte incorporated with LiBF_4 .

3.9. X-ray diffraction studies

X-ray diffraction is an analytical technique to examine the degree of amorphosity of polymer electrolytes, and to prove the complexation or interaction among polymers and inorganic salts. Fig. 9 illustrates the X-ray diffractograms of pure PAA, pure LiBF_4 , P80-L20, P75-L25, and P70-L30. The evidence of complexation among the constituents in the polymer electrolyte systems can be detected via changes in the peaks, such as shifting, shortening or broadening of peaks. [8]. In Fig. 9(a), nine sharp intense peaks are found at $2\theta = 21.2^\circ, 23.6^\circ, 26.7^\circ, 28.2^\circ, 31.9^\circ, 32.7^\circ, 36.3^\circ, 40.1^\circ,$ and 53.7° for LiBF_4 . Fig. 9(b) demonstrates four sharp peaks at $2\theta = 13.5^\circ, 17.0^\circ, 18.6^\circ,$ and 30.2° for PAA. Both disclose the crystalline character of PAA and LiBF_4 .

The PAA crystalline peaks at $2\theta = 13.5^\circ, 17.0^\circ, 18.6^\circ,$ and 30.2° disappeared in PAA- LiBF_4 electrolytes. The absence of the peaks demonstrates that lithium salt complexed with PAA while PAA has effectively solvate the lithium cations to achieve complete dissolution. As illustrated in Fig. 9(c)–(e), the diffraction peaks corresponding to LiBF_4 decreases. The reduction in peak intensity upon incorporation of LiBF_4 confirms the occurrence of complexation. Shifting of the peaks is observed upon inclusion of LiBF_4 . The peak shifting further confirms the complexation between PAA and LiBF_4 .

Among all the polymer electrolytes, the peaks of P80-L20 are slightly sharper than P70-L30. This reveals that P70-L30 exhibits higher degree of amorphosity. P70-L30 also indicates a broader peak at $2\theta = 20.3^\circ$ which suggests increases in amorphosity and thus leading to higher ionic conductivity. The increase in amorphosity in polymer electrolytes initiates the ionic hopping mechanism which leads to the improvement in the ionic conductivity [32]. The observations signify that the incorporation of lithium salt disrupts the orderly arrangement of polymer matrices. The degree of crystallinity is reduced and in other words the amorphous character increases. Higher loading of lithium salt reveals a higher amorphous degree which improves the ionic transportation in the polymer electrolyte systems leading to higher ionic conductivity.

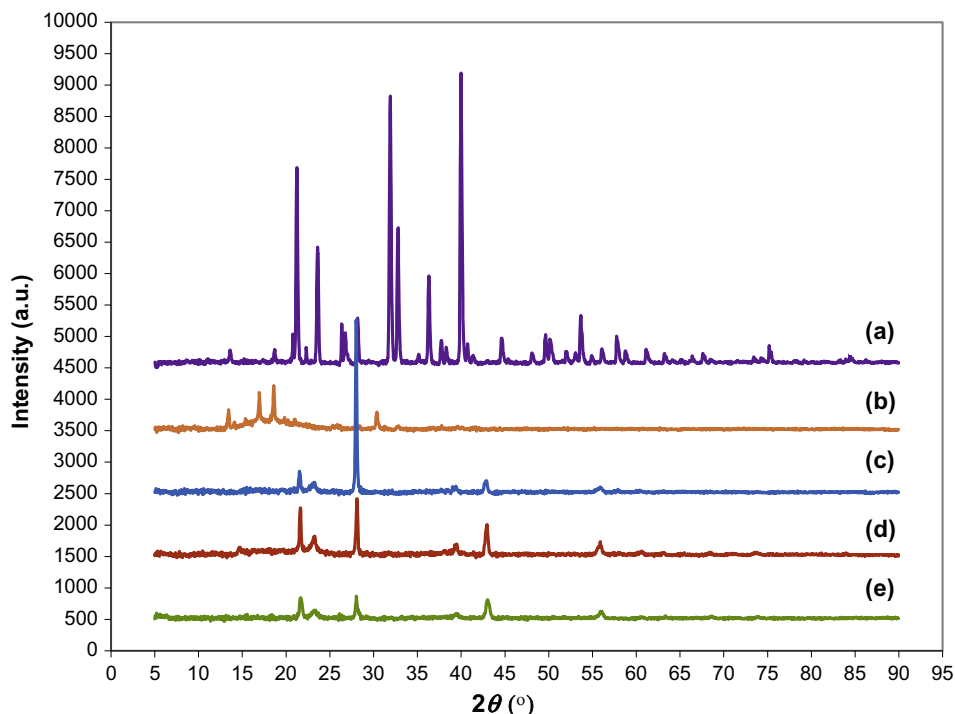


Fig. 9. XRD pattern of (a) pure LiBF_4 , (b) pure PAA, (c) P80-L20, (d) P75-L25, and (e) P70-L30.

4. Conclusion

In summary, polymer electrolytes with PAA and LiBF_4 were prepared by a solution casting method. The electrochemical properties of the PAA-based electrolyte systems were studied by means of AC-impedance spectroscopy. The highest ionic conductivity of $6.6 \times 10^{-4} \text{ S cm}^{-1}$ was achieved by addition of 30 wt% LiBF_4 . The results indicate that the electrochemical properties of the polymer electrolytes depend on the composition of the electrolyte systems. The network interactions between the lithium salt and polymer chains are formed easily and create a continuously network of conduction pathways. As a result, the electrochemical performance of the polymer electrolytes is improved. The E_a for the polymer systems is at the order of $10^{-2} \text{ kJ mol}^{-1}$. The dielectric permittivity studies demonstrated that as the lithium salt content in the polymer electrolytes increases, the number of charge carriers and stored charge also increase. The dielectric modulus studies indicated that all the tested polymer electrolytes have high capacitive values. A wider window of electrochemical stability has been observed. It is concluded that the polymer electrolytes have better electrochemical stability. By analyzing the thermal stability of the polymer electrolytes via TGA, it can be seen that P80-L20 exhibits better thermal stability compared to P70-L30 and L85-L25. The disappearance of peaks and reduction in peak intensity demonstrated in XRD analysis show the increase in the amorphous fraction in the polymer electrolytes. This work provides a promising method to develop polymer electrolytes with enhanced performance for potential applications in electrical devices.

Acknowledgements

This work was supported by the Fundamental Research Grant Scheme (FP012-2015A) from the Ministry of Higher Education Malaysia, University of Malaya and Postgraduate Research Grant (PG120-2015B) and Grand Challenges Grant (GC002A15SBS).

References

- [1] J.R. MacCallum, C.A. Vincent, *Polymer Electrolytes Reviews*, vol. 2, Elsevier, London, 1987.
- [2] B. Scrosati, *Applications of Electroactive Polymers*, Chapman Hall, London, 1993.
- [3] D.E. Fenton, J.M. Parker, P.V. Wright, Complexes of alkali metal ions with poly(ethylene oxide), *Polymer* 14 (1973) 589.
- [4] C.A. Vincent, *Polymer electrolytes*, *Prog. Solid State Chem.* 17 (1987) 145–261.
- [5] N.N. Saadun, S. Ramesh, K. Ramesh, Development and characterization of poly(1-vinylpyrrolidone-co-vinyl acetate) copolymer based polymer electrolytes, *Sci. World J.* (2014) 254215.
- [6] M.A.B.H. Susan, T. Kaneko, A. Noda, M. Watanabe, Ion gels prepared by in situ radical polymerization of vinyl monomers in an ionic liquid and their characterization as polymer electrolytes, *J. Am. Chem. Soc.* 127 (2005) 4976–4983.
- [7] J.Y. Sanchez, F. Alloinand, C.P. Lepmi, Polymeric materials in energy storage and conversion, *Mol. Cryst. Liq. Cryst.* 324 (1998) 257–266.
- [8] S. Ramesh, S.C. Lu, Enhancement of ionic conductivity and structural properties by BMIMTF ionic liquid in P(VdF-HFP)-based polymer electrolytes, *J. Appl. Polym. Sci.* 126 (2012) 484–492.
- [9] J.H. Kim, M.S. Kang, Y.J. Kim, J. Won, N.G. Park, Y.S. Kang, Dye-sensitized nanocrystalline solar cells based on composite polymerelectrolytes containing fumed silica nanoparticles, *Chem. Commun.* 14 (2004) 1662–1663.
- [10] F. Croce, L. Persi, B. Scrosati, F. Serraino-Fiory, E. Plichta, M.A. Hendrickson, Role of the ceramic fillers in enhancing the transport properties of composite polymer electrolytes, *Electrochim. Acta* 46 (2001) 2457–2461.
- [11] J.E. Weston, B.C.H. Steele, Effects of inert fillers on the mechanical and electrochemical properties of lithium salt-poly(ethylene oxide) polymer electrolytes, *Solid State Ionics* 7 (1983) 75–79.
- [12] M. Alamgir, K. Abraham, Li ion conductive electrolytes based on poly(vinyl chloride), *J. Electrochem. Soc.* 140 (1993) L96–L97.
- [13] M. Sukeshini, A. Nishimoto, M. Watanabe, Transport and electrochemical characterization of plasticized poly(vinyl chloride) solid electrolytes, *Solid State Ionics* 86 (1996) 385–393.
- [14] K. Tsunemi, H. Ohno, E. Tsuchida, Mechanism of ionic conduction of PvdF-lithium perchlorate hybrid films, *Electrochim. Acta* 28 (1983) 833–837.
- [15] H.S. Choe, J. Giaccari, M. Alamgir, K.M. Abraham, Preparation and characterization of poly(vinyl sulfone) and poly(vinylidene fluoride)-based electrolytes, *Electrochim. Acta* 40 (1995) 2289–2293.
- [16] J. Vondrak, M. Sedlarikova, J. Velicka, B. Klapste, V. Novak, J. Reiter, Gel polymer electrolytes based on PMMA, *Electrochim. Acta* 46 (2001) 2047–2048.
- [17] H.J. Rhoo, H.T. Kim, J.K. Park, T.S. Hwang, Ionic conduction in plasticized PVC/PMMA blend polymer electrolytes, *Electrochim. Acta* 42 (1997) 1571–1579.
- [18] W. Kam, C.W. Liew, J.Y. Lim, S. Ramesh, Electrical, structural, and thermal studies of antimony trioxide-doped poly(acrylic acid)-based composite polymer electrolytes, *Ionics* 20 (2014) 665–674.

- [19] A. Arslan, S. Kiralp, L. Toppare, A. Bozkurt, Novel conducting polymer electrolyte biosensor based on poly(1-vinylimidazole) and poly(acrylic acid) networks, *Langmuir* 22 (2006) 2912–2915.
- [20] Y. Zhu, S. Xiao, Y. Shi, Y. Yang, Y. Wu, A trilayer poly(vinylidene fluoride)/polyborate/ poly(vinylidene fluoride) gel polymer electrolyte with good performance for lithium ion batteries, *J. Mater. Chem. A* 1 (2013) 7790–7797.
- [21] J.H. Shin, Y.T. Lim, K.W. Kim, H.J. Ahn, J.H. Ahn, Effect of ball milling on structural and electrochemical properties of (PEO)_nLiX (LiX = LiCF₃SO₃ and LiBF₄) polymer electrolytes, *J. Power Sources* 107 (2002) 103–109.
- [22] A.M. Stephan, N.G. Renganathan, T.P. Kumar, R. Thirunakaran, S. Pitchumani, J. Shrisudersan, N. Muniyandi, Ionic conductivity studies on plasticized PVC/PMMA blend polymer electrolyte containing LiBF₄ and LiCF₃SO₃, *Solid State Ionics* 130 (2000) 123–132.
- [23] C.W. Liew, S. Ramesh, R. Durairaj, Impact of low viscosity ionic liquid on PMMA PVC LiTFSI polymer electrolytes based on Ac impedance, dielectric behavior and HATR FTIR characteristics, *J. Mater. Res.* 27 (2012) 2996–3004.
- [24] A. Awadhia, S.K. Patel, S.L. Agrawal, Dielectric investigations in PVA based gel electrolytes, *Prog. Cryst. Growth Charact. Mater.* 52 (2006) 61–68.
- [25] M.H. Buraidah, L.P. Teo, S.R. Majid, A.K. Arof, Ionic conductivity by correlated barrier hopping in NH₄I doped chitosan solid electrolyte, *Physica B* 404 (2009) 1373–1379.
- [26] M.C.R. Shastry, K.J. Rao, Ac conductivity and dielectric relaxation studies in AgI-based fast ion conducting glasses, *Solid State Ionics* 44 (1991) 187–198.
- [27] S.A. Suthanthiraraj, D.J. Sheeba, B.J. Paul, Impact of ethylene carbonate on ion transport characteristics of PVdF–AgCF₃SO₃ polymer electrolyte system, *Mater. Res. Bull.* 44 (2009) 1534–1539.
- [28] R. Kotz, M. Carlen, Principles and applications of electrochemical capacitors, *Electrochim. Acta* 45 (2000) 2483–2498.
- [29] C.W. Liew, S. Ramesh, Comparing triflate and hexafluorophosphate anions of ionic liquids in polymer electrolytes for supercapacitor applications, *Materials* 7 (2014) 4019–4033.
- [30] M.C. McGaugh, S. Kottle, The thermal degradation of poly(acrylic acid), *J. Polym. Sci. Part C: Polym. Lett.* 5 (1967) 817–820.
- [31] A. Gurkaynak, F. Tubert, J. Yang, J. Matyas, J.L. Spencer, C.C. Gryte, High-temperature degradation of polyacrylic acid in aqueous solution, *Polym. Chem.* 34 (1996) 349–355.
- [32] S. Ramesh, C.W. Liew, Development and investigation on PMMA-PVC blend-based solid polymer electrolytes with LiTFSI as dopant salt, *Polym. Bull.* 70 (2013) 1277–1288.